Tellus (1991), *43A*, 168–176

On the behavior of outflows with low potential vorticity from a sea strait

By ATSUSHI KUBOKAWA, *Department of Geophysics, Faculty of Science, Tohoku University, Sendai 980, Japan*

(Manuscript received 9 November 1989; in final form 21 March 1990)

ABSTRACT

Behavior of outflows from a sea strait contained in a shallow upper layer is investigated by using a simple quasigeostrophic model. The outflow is assumed to have two piecewise-uniform potential vorticities and the higher one to be the same value as that in the open ocean. It is shown that this simple model can reproduce both the gyre mode and the coastal mode similar to those observed near the Tsugaru Strait, which connects the Sea of Japan with the North Pacific, and in laboratory experiments. In addition to these two modes, a coastal mode in which the current at the downstream temporally widens can also occur in the present model. The existence of these three modes can be attributed to the limited capacity of the downstream coastal current to advect the low potential vorticity fluid and the characteristics of frontal waves. The responses of the flow pattern to the changes in the outflow conditions are also briefly examined.

1. Introduction

It is well-known that the outflows with low density from a sea strait can have two different modes; one is called the coastal mode in which the outflow forms a narrow jet clinging to the right-hand coast (in the northern hemisphere), and the other the gyre mode in which the outflow separates from the coast and forms an anticyclonic gyre. The existence of these two modes was first reported by Whitehead and Miller (1979) in their laboratory experiments which were carried out to simulate the gyre in the Alboran Sea. It is also known that the outflow from the Tsugaru Strait, which connects the Sea of Japan with the North Pacific (see Fig. 1), takes both the coastal mode and the gyre mode (Conlon, 1982). The gyre mode appears from summer to autumn and in the other seasons the current flows along the coast. Conlon discussed the seasonal variability of this current based on the results of Whitehead and Miller (1979) (see also Ichiye, 1982). Laboratory experiments using a model whose geometry resembles that around the Tsugaru Strait were carried out by Kawasaki and Sugimoto (1984).

The recent spread of the satellite infrared images has made it possible to investigate the detailed structure of the outflow pattern and its variability. Yasuda et al. (1988) studied the variability of the Tsugaru Warm Current in autumn, and found a quasi-periodic variation in the outflow pattern with a period of 20–30 days. They suggested that this variation could be attributed to a change in the outflow rate. A laboratory experiment for variable outflow rate was carried out by Kawasaki and Sugimoto (1988), and a similar cycle of the outflow pattern was obtained, while the phase relationship between the outflow pattern and the outflow rate seems different from observation.

Although there are observational reports and experimental studies as mentioned above, the dynamics of this phenomenon remains unclear. The difficulty in theoretical treatment arises from the nonlinear nature of the problem. If we deal with this problem using linearized shallow water equations, the outflow forms a coastal current flowing along a right-hand coast after geostrophic adjustment as demonstrated by Minato (1983). Nonlinear stationary paths of the outflows were examined by Nof (1978, 1987). Nof (1978) considered the effect of a sudden widening in a channel and showed that outflow with anticyclonic shear can be deflected to the left. This result strongly suggests that the potential vorticity is an impor-

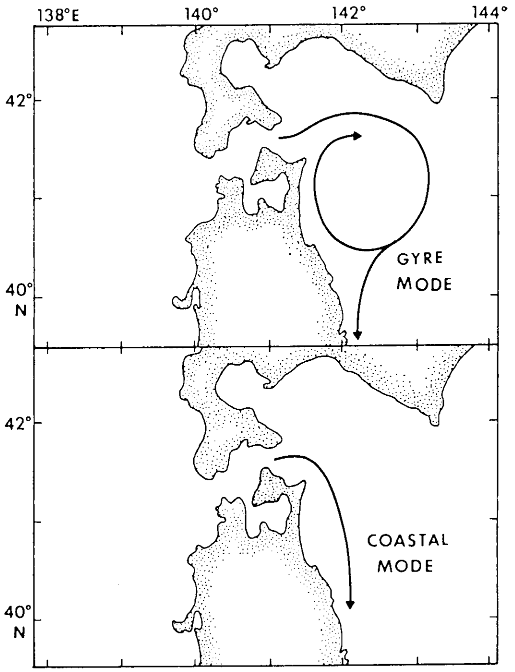

Fig. 1. Schematic representation of principal modes of outflow jet from the Tsugaru Strait. (Adapted from Conlon, 1982).

tant factor for determining the outflow pattern. On the other hand, Nof (1987) examined the effect of the shape of the oceanic basin, under the conditions that the strait is narrower than the deformation radius, and that the Rossby number in which the width of the strait is used as the length scale, is larger than unity.

In the present study, we focus our attention on the effect of the potential vorticity distribution. The shallow water equations in which no isopycnal intersects the sea surface is adopted as in the above theoretical studies, and the width of the strait is assumed to have the scale of the deformation radius, since the Tsugaru Strait has this scale. The time-dependency is also included. By assuming small Rossby number, the equations can be reduced to a quasigeostrophic potential vorticity equation with a coastal current, and we treat it under the condition that the model ocean consists of two piecewise uniform potential vorticity regions.

After formulating the problem in Section 2, the necessary condition for the formation of steady coastal currents and that for the gyre formation are presented in Section 3. It is shown in Section 4, with aid of numerical computations using a contour dynamics method (e.g. Zabusky et al., 1979; Pratt and Stern, 1986), that these conditions uniquely determine the outflow pattern when the fluid is initially at rest. The response of the outflow pattern to the change in the outflow conditions at the outlet are briefly examined. The results are summarized in Section 5, and brief discussions on the applicability of the present results are given.

2. Model configuration and formulation

Let us consider the model configuration shown in Fig. 2, in which the motion is concentrated in the shallow upper layer and the lower layer is assumed to be very deep and passive. The vertical coast exists at $y=0$, and the shelf slope is neglected. Although the density in the active layer is constant,

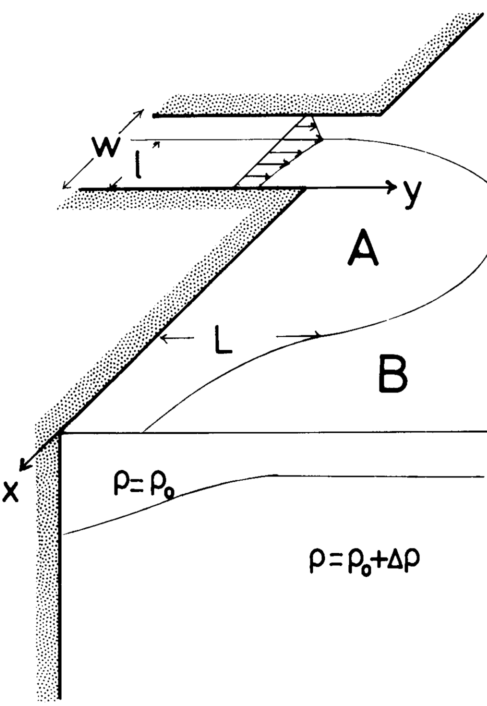

Fig. 2. Model configuration. The model consists of two piecewise-uniform potential vorticity regions. The potential vorticity in region A is assumed to be lower than that in B.

a fluid with low potential vorticity might be regarded as a low-density fluid in the real ocean and in the experiments, since the low-density fluid tends to depress the interface and to form an anticyclonic circulation. When viscosity and diffusion are neglected, the governing equations are

$$\boldsymbol{u}_t + \boldsymbol{u} \cdot \nabla \boldsymbol{u} + f\boldsymbol{k} \times \boldsymbol{u} = -g' \nabla h, \tag{2.1}$$

$$h_t + \nabla \cdot \{(h+H)\boldsymbol{u}\} = 0, \tag{2.2}$$

where $\boldsymbol{u}$ is the horizontal velocity vector (u, v), H the thickness of the active (upper) layer at $y = \infty$, h the departure of the layer thickness from H, t the time, ∇ the horizontal differential operator (∂_x, ∂_y), f the Coriolis parameter, $\boldsymbol{k}$ the unit vector positive upward and g' is the reduced gravity $(= \Delta\rho g \rho_0^{-1})$.

Since the width of strait is assumed to have the scale of the deformation radius $L_R = f^{-1}(g'H)^{1/2}$, we can choose L_R as the horizontal scale of the system. However, for the time being, there are two characteristic scales; one of them is f^{-1} and the other is the advection time scale, $L_R U^{-1}$, where U is the typical current velocity. If we assume $L_R U^{-1} \gg f^{-1}$, i.e., the Rossby number $\varepsilon = U(fL_R)^{-1}$ is much smaller than unity, h/H becomes $O(\varepsilon)$. In this case, we can introduce multiple time scales, and the governing equations (nondimensionalized by using f, U, H and L_R) become:

$$\boldsymbol{u}_t + \boldsymbol{k} \times \boldsymbol{u} + \nabla h + \varepsilon\{\boldsymbol{u}_T + \boldsymbol{u} \cdot \nabla \boldsymbol{u}\} = 0, \tag{2.3}$$

$$h_t + \nabla \cdot \boldsymbol{u} + \varepsilon\{h_T + \nabla \cdot (h\boldsymbol{u})\} = 0, \tag{2.4}$$

where t and T denote the times with the scales of f^{-1} and $L_R U^{-1}$, respectively. The boundary conditions are

$$v(x, 0, t, T) = v_b(x, T), \tag{2.5a}$$

$$(h, u, v) \to (0, 0, 0) \quad \text{as} \quad y \to \infty, \tag{2.5b}$$

where v_b is the offshore velocity at the outlet of the strait.

Since our interest is in phenomena with a timescale much longer than f^{-1}, we may drop the terms with t-derivative, and this procedure leads the quasigeostrophic potential vorticity equation (see Pedlosky, 1979). However, in this case, the boundary condition at the coast, i.e., h at $y = 0$, cannot be determined because of the geostrophic degeneracy. In order to determine it, we should also treat the dynamics with the time scale f^{-1}.

Expanding the dependent variables in powers of ε, we obtain the following equations to the lowest order:

$$\boldsymbol{u}_t^{(0)} + \boldsymbol{k} \times \boldsymbol{u}^{(0)} + \nabla h^{(0)} = 0, \tag{2.6}$$

$$h_t^{(0)} + \nabla \cdot \boldsymbol{u}^{(0)} = 0, \tag{2.7}$$

where the superscript $^{(0)}$ denotes the lowest order quantities in the expansion. From these equations, it can easily be found that the potential vorticity $q = v_x^{(0)} - u_y^{(0)} - h^{(0)}$ is independent of t. If we divide $\boldsymbol{u}^{(0)}$ and $\boldsymbol{h}^{(0)}$ into two parts:

$$\begin{aligned} \boldsymbol{u}^{(0)} &= \boldsymbol{u}_K(x, y, t; T) + \boldsymbol{u}_G(x, y, T), \\ h^{(0)} &= h_K(x, y, t; T) + h_G(x, y, T), \end{aligned} \tag{2.8}$$

the boundary conditions at the coast for variables with subscript K and G may be chosen as:

$$v_K(x, 0, t; T) = v_b(x, T), \tag{2.9a}$$

$$h_G(x, 0, T) = 0; \tag{2.9b}$$

they also satisfy

$$v_{Kx} - u_{Ky} - h_K = 0, \tag{2.10a}$$

$$v_{Gx} - u_{Gy} - h_G = q(x, y, T), \tag{2.10b}$$

$$\boldsymbol{u}_G = \boldsymbol{k} \times \nabla h_G. \tag{2.10c}$$

The equations for $\boldsymbol{u}_K$ and $\boldsymbol{h}_K$ give the distribution of $h^{(0)}$ at the coast; they were solved by Minato (1983) as an initial value problem. The solution of this problem displays the propagation of the Kelvin wave, and for $t \gg 1$, a steady geostrophic flow along the right-hand coast is formed:

$$h_K(x, y, t \to \infty; T) = \frac{y}{\pi} \int_{-\infty}^{\infty} d\xi \, \frac{1}{\zeta} \times K_1(\zeta) \int_{-\infty}^{\xi} d\xi' v_b(\xi', T), \tag{2.11a}$$

$$\boldsymbol{u}_K(x, y, t \to \infty; T) = \boldsymbol{k} \times \nabla h_K(x, y, t \to \infty; T), \tag{2.11b}$$

where $\zeta = \{(x-\xi)^2 + y^2\}^{1/2}$ and K_1 is the modified Bessel function of the second kind of order 1.

To next order in ε, we can obtain a quasi-geostrophic potential vorticity equation for the advection time scale:

$$q_T + J(\psi, q) = 0, \tag{2.12}$$

where $J(\psi, *)$ is the Jacobian operator and ψ is the geostrophic stream function

$$\psi(x, y, T) = h_K(x, y, t \to \infty; T) + h_G(x, y, T),$$

and the potential vorticity can be written as

$$q = \nabla^2\psi - \psi.$$

This equation with the boundary conditions,

$$\psi(x, 0, T) = h_K(x, 0, t \to \infty; T) = \int_{-\infty}^{x} d\xi v_b(\xi, T), \tag{2.13a}$$

$$\psi(x, y \to \infty, T) = 0, \tag{2.13b}$$

governs the evolution of outflows.

In the present article, we treat (2.12) with (2.13a, b) for a simple two piecewise uniform potential vorticity distribution shown in Fig. 2 ($q = -P$ in region A and 0 in region B). In the strait, q is assumed to be

$$q = \begin{cases} -P & \text{for} \quad -l < x < 0, \\ 0 & \text{for} \quad -w < x < -l, \end{cases} \tag{2.14}$$

where w is the width of the strait, and this yields

$$\psi(x, 0, T) = \begin{cases} 0 & \text{for} \quad x \leqslant -w, \\ \dfrac{h_0 + P\{\cosh l - 1\}}{\sinh w} \sinh(x + w) & \\ h_0 & \text{for} \quad x \geqslant 0, \end{cases}$$
$$- \begin{cases} 0 & \text{for} \quad -w < x \leqslant -l, \\ P\{\cosh(x + l) - 1\} & \text{for} \quad -l < x < 0, \end{cases} \tag{2.13a'}$$

where h_0 is the total transport of the outflow. Although this choice of the potential vorticity distribution at the strait seems too artificial, it makes it possible to get a simple and clear idea of the cause of the occurrence of various outflow modes.

3. Necessary conditions for steady coastal mode and gyre formation

Before solving (2.12) with (2.13) numerically in Section 4, let us consider the conditions for formation of a steady coastal current or anticyclonic gyre.

For a steady outflow condition, it can be expected that the y-coordinate of the potential vorticity front (the discontinuous surface of the potential vorticity), $L(x, T)$, is almost independent of x at a far downstream position. Therefore, the stream function there becomes

$$\psi(x \to \infty, y, T) = \{h_0 + P(\cosh L - 1)\} e^{-y} - \begin{cases} P\{\cosh(L - y) - 1\} & \text{for} \quad y < L, \\ 0 & \text{for} \quad y \geqslant L. \end{cases} \tag{3.1}$$

If the current is steady, the transport of the low potential vorticity fluid (LPVF hereafter) far downstream should coincide with that in the strait, i.e.,

$$\psi(x \to \infty, L, T) = \psi(-l, 0, T). \tag{3.2}$$

This condition is not always satisfied, e.g., if l coincides with w, it is clear that (3.2) is not satisfied unless $P = 0$. In other words, the capacity of the coastal current to advect the LPVF is limited. From (3.1), we can easily find that the maximum value of the ratio of LPVF to the total transport, $1 - \psi(x, L, T)/h_0$, far downstream is:

$$Q_{Rc} = \begin{cases} 1 - P/2h_0 & \text{for} \quad P/h_0 < 1, \\ h_0/2P & \text{for} \quad P/h_0 \geqslant 1. \end{cases} \tag{3.3a}$$

Therefore, for the steady coastal mode to occur, this ratio in the strait,

$$Q_R = 1 - \psi(-l, 0, T)/h_0, \tag{3.3b}$$

should satisfy the inequality

$$Q_R \leqslant Q_{Rc}. \tag{3.3c}$$

When (3.3c) is not satisfied, the current width near the strait will become wide, since the outflow rate of LPVF exceeds the transport capacity of the downstream current. In this situation, if the frontal wave, i.e., disturbances in $L(x, t)$, propagates upstream, the LPVF will stagnate near the outlet and will establish the anticyclonic gyre. Since the downstream phase speed of short frontal waves is always higher than the longwave phase speed (see Pratt and Stern, 1986), the longwave speed will divide the unsteady outflow patterns into the two categories. The propagation speed of the long frontal wave (see Stern, 1986) is

$$c = \{h_0 - P(1 - e^{-L})\} e^{-L}. \tag{3.4}$$

Therefore, if $P/h_0 > 1$ and $L > \ln(1 - h_0/P)^{-1}$, the long frontal wave propagates in the negative x direction. If L is sufficiently small, c is always positive. However, if $Q_R > Q_{Rc}$, since L increases with time, c will turn to be negative at some time in the case of $P/h_0 > 1$, and the anticyclonic gyre will be formed.

From the above considerations, we can expect that there are three outflow modes determined by the values of P/h_0 and Q_R:

(I)	$Q_R < Q_{Rc}$; steady coastal mode,	
(II)	$Q_R > Q_{Rc}$, $P/h_0 \leq 1$; widening coastal mode,	(3.5)
(III)	$Q_R > Q_{Rc}$, $P/h_0 > 1$; gyre mode.	

When $Q_R = Q_{Rc}$, the steady coastal mode will also occur for $P/h_0 > 1$ but not for $P/h_0 \leq 1$, since L in (3.1) becomes infinite in the latter case. It should also be noted here that only when $P/h_0 > 1$, is the return flow (toward negative x direction) near the coast possible (see (3.1)).

4. Numerical results

In order to verify the above expectations, numerical computations have been carried out by the contour dynamics method. This method has become quite standard, so that we will not describe it in detail (see, e.g., Zabusky et al., 1979; Pratt and Stern, 1986). The only difference from the ordinary contour dynamics method is the existence of the coastal current, (u_K, v_K). This current component can be represented from (2.11a, b) in integral form:

$$u_K = -\frac{1}{\pi}\int_{-\infty}^{\infty} d\xi \frac{1}{\zeta^3} \{(\zeta^2 - 2y^2) K_1(\zeta) - \zeta y^2 K_0(\zeta)\} \psi(x, 0, T), \tag{4.1}$$

$$v_K = \frac{y}{\pi}\int_{-\infty}^{\infty} d\xi \frac{x-\xi}{\zeta^3} \{2K_1(\zeta) - \zeta K_0(\zeta)\} \psi(x, 0, T), \tag{4.2}$$

where $\zeta = \{(x-\xi)^2 + y^2\}^{1/2}$. Since $|v_K| \ll 1$ except near the strait, $u_K = h_0 e^{-y}$ and $v_K = 0$ were used for $x > 5$. The movement of particles on the potential vorticity front is governed by

$$\frac{dL}{dT} = v_K(x, L, T) + v_G(x, L, T), \tag{4.3}$$

$$\frac{dx}{dT} = u_K(x, L, T) + u_G(x, L, T), \tag{4.4}$$

where (u_G, v_G) are solutions of (2.10b, c), with the boundary conditions (2.5b) and (2.9b) and their integral forms given in Stern (1986). Using these equations, we can numerically calculate the temporal evolution of $L(x, T)$.

In the present study, the particles were added to keep the interval between $(-l, 0)$ and the adjacent particle sufficiently small, and were removed when they were beyond $x = 8$. For $x > 7.5$, the particles were assumed to be advected by the x-independent current velocity given by (3.1). The changes in L far downstream are caused only by the propagation of frontal waves. This means that if the propagation direction of a frontal wave at large x is initially positive, it remains positive or zero unless h_0 is reduced. Therefore, it is expected that the downstream conditions hardly affect the evolution near the strait.

P/h_0 and Q_R used in this study are plotted in Fig. 3, in which the boundaries of three regimes of the flow patterns expected in Section 3 are also drawn. The initial condition imposed on these computations is $L(x, 0) \ll 1$, and the evolution of $L(x, T)$ in all the cases was in line with expectations. Typical results in the three regimes can be found in Fig. 4.

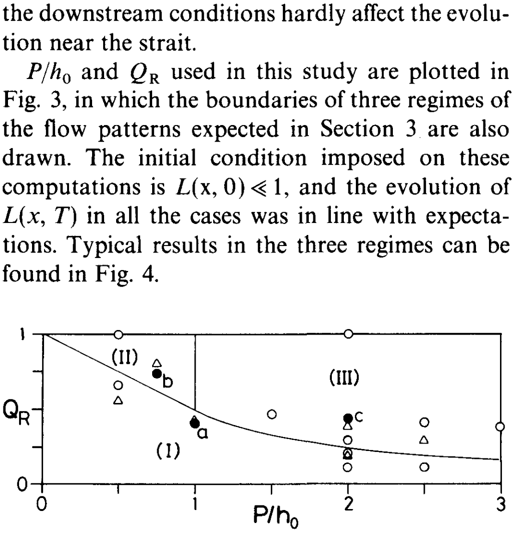

Fig. 3. Three regimes of the $P/h_0 - Q_R$ plane, and parameters used in numerical computations. The circles and triangles denote the parameters used in the numerical computations with $w = 1.0$ and $w = 1.5$, respectively, and the solid curves in this panel are the boundaries of the regimes. For letters (a), (b) and (c), see Fig. 4.

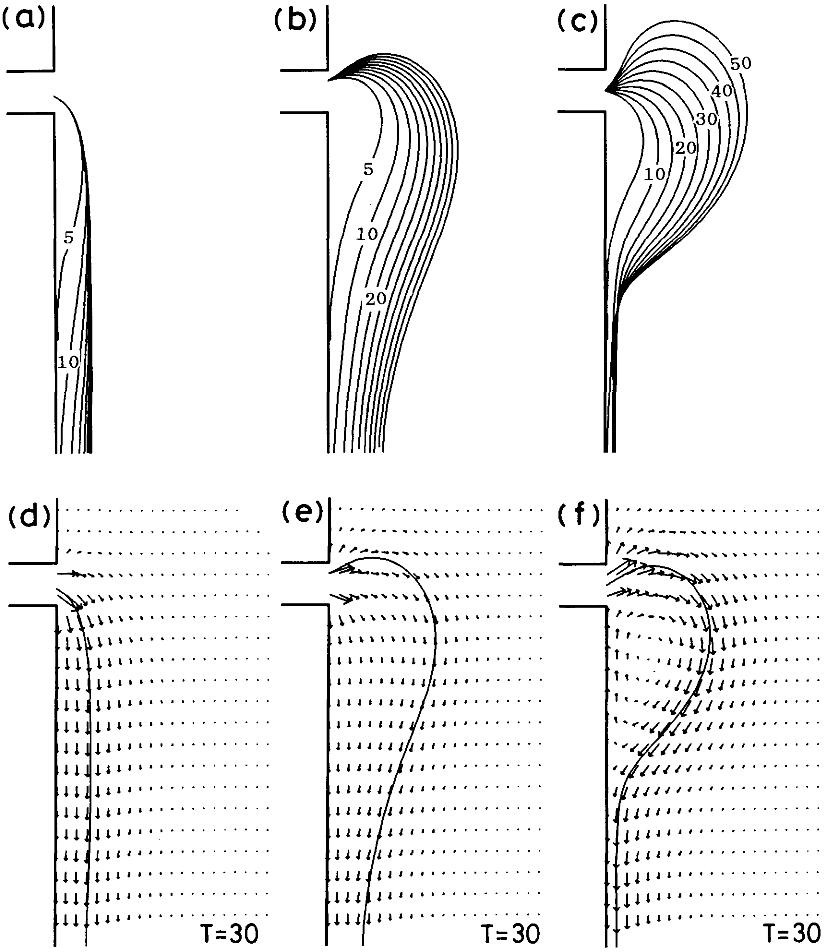

Fig. 4. The typical results in the three regimes, (I), (II) and (III). Panels (a)–(c) show the temporal evolutions of the frontal positions, with the parameters at the closed circles having letters (a)–(c) attached in Fig. 3 (numerals denote T). Panels (d)–(f) show the current vectors at $T = 30$ in these cases. In the numerical computations, h_0 is normalized to be 1.0.

In regime (I), LPVF forms a narrow steady coastal current, while in regime (II) the potential vorticity front continues to move offshore. In regime (III), LPVF forms an anticyclonic gyre near the outlet and tends to extend in the $-x$ direction. This extension is caused by the mirror image of the coastal boundary. When $l = w$, in both the regimes (II) and (III), the front propagates in the $-x$ direction along the coast as shown in Fig. 5, since LPVF cannot separate from the left coast and the mirror image advects it. However, in this case, the offshore width of LPVF in regime (II) continues to enlarge and evolves in a different way of that in regime (III).

In the present formulation, since v_b is a function of T, the response of LPVF to the change in the outflow condition can be examined. Two examples of the responses are shown in Fig. 6, in which we have chosen the distribution of LPVF at $T = 30$ in panel (c) of Fig. 4 as the initial value. In panel (a), h_0 is increased, while l in (2.13a′) is fixed. In this case, the LPVF pool is advected downstream and

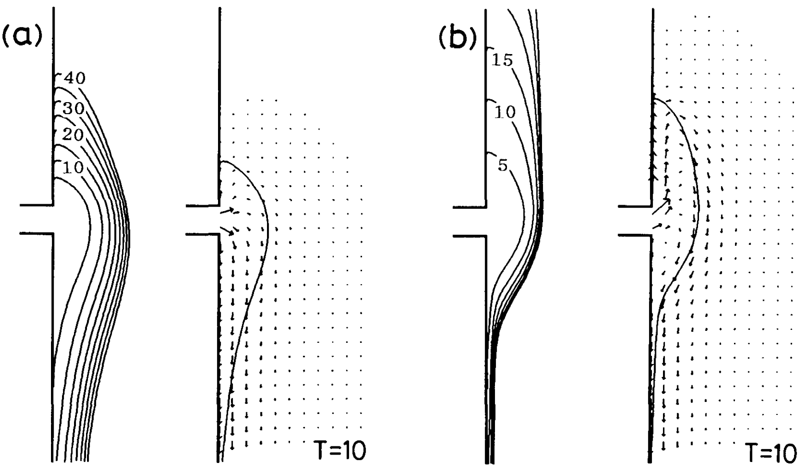

Fig. 5. Temporal evolution of the cases in which $w = 1.0$ and $Q_R = 1.0$; (a) $P/h_0 = 0.5$ and (b) $P/h_0 = 2.0$.

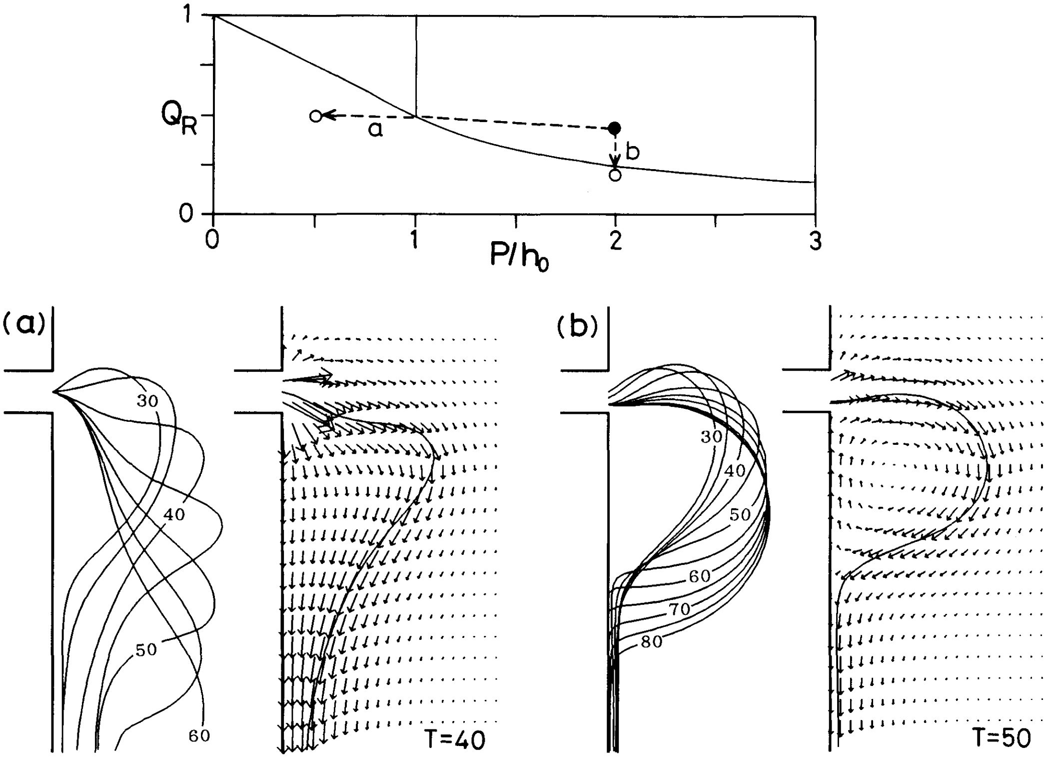

Fig. 6. Responses of the anticyclonic gyre shown in Fig. 4f to the changes in the outflow conditions along the broken lines in the upper panel; (a) h_0 is linearly increased from 1.0 to 4.0 in the period from $T = 30$ to 40 but l is fixed (corresponding change in P/h_0 is from 2.0 to 0.5 and Q_R slightly increases); (b) l is linearly reduced from 0.5 to 0.2 in the same period (the corresponding change in Q_R is from 0.443 to 0.214). For $T \geq 40$, the parameters are fixed at their terminal values.

the coastal current is swiftly formed near the strait. On the other hand, in panel (b), in which h_0 is fixed and l is reduced, the gyre rotates in clockwise, and expands offshore. This clockwise rotation is explainable from the rotating tendency of elliptical eddies; the axes of elliptical eddies with anticyclonic vorticity tend to rotate in an anticyclonic direction (Lamb, 1932; Cushman-Roisin et al., 1985).

The computation of panel (b) in Fig. 6 was continued to $T = 160$, but this LPVF pool did not disappear. While Q_R is smaller than Q_{Rc}, the anticyclonic gyre blocks the downstream LPVF flow, and further stagnation of LPVF occurs. However, in another case, in which the LPVF distribution at $T = 5$ in Fig. 4(b) was chosen as the initial value, the coastal current formation near the strait was observed (not shown here). These results suggest that the evolution of the flow pattern also depends on the initial value.

5. Summary and discussion

In the present article, we have examined the behavior of low potential vorticity fluid debouching from a sea strait, and have shown that the outflow takes the three different modes. The existence of these modes can be attributed to the limited capacity of the coastal current to advect the low potential vorticity fluid and the characteristics of frontal waves.

Since the dynamics in the strait has been excluded in the present model, the outflow pattern does not depend explicitly on the width of the strait. However, if it is assumed that the current flows in a positive y direction everywhere in the strait, possible values of Q_R and P/h_0 depend on the width of the strait, w. From (2.13a′), we can easily find that for v_b positive everywhere,

$$\frac{h_0}{P} - 1 + \frac{\cosh(w-l)}{\cosh w} > 0.$$

This equation gives the maximum value of l, or equivalently Q_R, for given values of w and P/h_0. Fig. 7 shows the maximum value of Q_R under this condition as a function of P/h_0 for various value of w. From this figure, it is expected that the gyre mode hardly occurs when the strait is wider than the Rossby radius of deformation.

As mentioned in Section 1, the problem treated here is closely related to the Tsugaru Warm Current. The seasonal selection of the outflow mode has been thought to be caused by the seasonal changes of the radius of deformation (Conlon, 1982) and the magnitude of the Rossby number (Ichiye, 1982; Kawasaki and Sugimoto, 1984). The present model is constructed under the small Rossby number limit, and the potential vorticity distribution is the most important factor. The *Rossby number* in the experiment by Kawasaki and Sugimoto (1984) might correspond to the strength of the anticyclonic shear, and if so, the present model results are consistent. However, in the present stage, the relation between the *Rossby number* and the strength of anticyclonic shear or the potential vorticity is unknown. The seasonal variation of the potential vorticity of the outflow should also be investigated to clarify this problem.

The recent observation by Yasuda et al. (1988) revealed that the Tsugaru Warm Gyre changes with a period from 20 days to 1 month. In their paper, it is suggested that the warm water pool rotates in a clockwise direction when the outflow rate estimated from the sea level differences around the strait decreases; the warm water pool expands offshore as a result. This behavior seems resemble to that in Fig. 6(b) in which Q_R is decreased. Interaction between the gyre and the coastal current similar to that in our model may occur in the Tsugaru Warm Gyre, although the gyre in the present model tends to enlarge continuously even if Q_R is decreased. For the observed cyclic feature of the warm gyre, the shelf slope might be important,

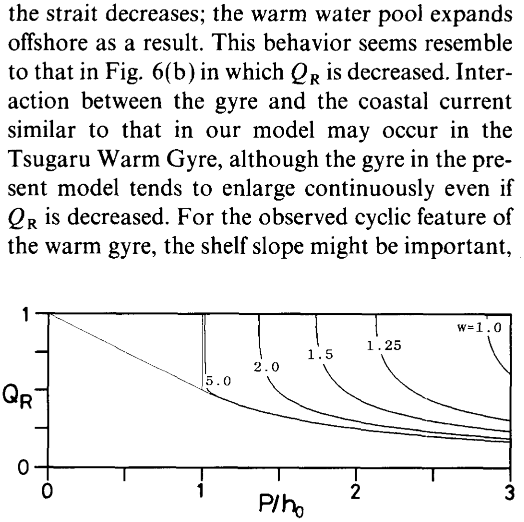

Fig. 7. The maximum values of Q_R as a function of P/h_0 for various width of the strait, w, under the condition that the current in the strait flows in a positive y direction everywhere (thick curves with numerals). Thin curves denote the boundaries of the three regimes.

since the slope possibly permits the existence of a shelf wave-like coastal current which is hardly affected by the offshore potential vorticity distribution. In such a situation, the perfect blocking of the low potential vorticity fluid by the anticyclonic gyre observed in the present model (see Fig. 6b) may not occur, and its further stagnation might cease after Q_R is decreased below Q_{Rc}.

6. Acknowledgments

The author would like to extend his hearty thanks to Dr. K. Hanawa for his valuable comments on the manuscript. This study was supported by a Grant-in-Aid for Scientific Research from the Ministry of Education, Science and Culture, Japan.

REFERENCES

Conlon, D. M. 1982. On the outflow modes of the Tsugaru Warm Current. *La mer 20*, 60–64.

Cushman-Roisin, B., Hell, W. H. and Nof, D. 1985. Oscillations and rotations of elliptical warm-core rings. *J. Geophys. Res. 90*, 11756–11764.

Ichiye, T. 1982. A commentary note on the paper "On the outflow modes of the Tsugaru Warm Current" by D. M. Conlon. *La mer 20*, 125–128.

Kawasaki, Y. and Sugimoto, T. 1984. Experimental studies on the formation and degeneration processes of the Tsugaru warm gyre. In: *Ocean hydrodynamics of the Japan and East China Sea* (ed. T. Ichiye). D. Reidel Publ. Comp. 225–238.

Kawasaki, Y. and Sugimoto, T. 1988. A laboratory study of the short-term variation of the outflow pattern of the Tsugaru Warm Water with a change in its volume transport. *Bull. Tohoku Reg. Fish. Res. Lab. 50*, 203–215 (in Japanese with English abstract and captions).

Lamb, H. 1932. *Hydrodynamics, 6th edition.* Cambridge University Press. 738 pp.

Minato, S. 1983. Geostrophic response near coast. *J. Oceanogr. Soc. Japan 39*, 141–149.

Nof, D. 1978. On geostrophic adjustment in sea straits and wide estuaries. Part II: Two-layer system. *J. Phys. Oceanogr. 8*, 861–872.

Nof, D. 1987. The bifurcation of outflows. *J. Phys. Oceanogr. 17*, 37–52.

Pedlosky, J. 1979. *Geophysical fluid dynamics.* Springer-Verlag, 624 pp.

Pratt, L. J. and Stern, M. E. 1986. Dynamics of potential vorticity front and eddy detachment. *J. Phys. Oceanogr. 16*, 1099–1118.

Stern, M. E. 1986. On the amplification of convergences in coastal currents and the formation of "squirts". *J. Mar. Res. 44*, 403–421.

Whitehead, J. A. and Miller, A. R. 1979. Laboratory simulation of gyre in the Alboran Sea. *J. Geophys. Res. 84*, 3733–3742.

Yasuda, I., Okuda, K., Hirai, M., Ogawa, Y., Kudoh, H., Fukushima, S. and Mizuno, K. 1988. Short-term variations of the Tsugaru Warm Current in autumn. *Bull. Tohoku Reg. Fish. Res. Lab. 50*, 153–191 (in Japanese with English abstract and captions).

Zabusky, N. J., Hughes, M. and Roberts, K. V. 1979. Contour dynamics for the Euler equations in two dimensions. *J. Comput. Phys. 30*, 96–106.